**WOOD RESEARCH** doi.org/10.37763/wr.1336-4561/71.1.8092
**e-ISSN 2729-8906**
**71(1): 2026 80-92 pp.**

# AGING OF WOODEN COMPONENTS IN ANCIENT TIMBER STRUCTURES. FIRE RISK AND SMOKE-HEAT HAZARDS

TIANWEI ZHANG, MINGZE BAI, HAO LIU, ZIDONG GUO, ZHIXIN TANG,
HAO CHANG, XIAORUI ZHANG
CHINA PEOPLE'S POLICE UNIVERSITY
CHINA

(RECEIVED JANUARY 2026)

## ABSTRACT

Based on the aging characteristics of wooden components, this study adopted artificial accelerated aging and fire propagation apparatus (FPA) to examine how aging affects the combustion behaviour, fire risk, and smoke-heat hazards of pine wood commonly used in ancient structures. Wood specimens with dimensions (100×100×10 mm and 300×100×10 mm) matching fire performance tests were prepared, and artificial accelerated photoaging treatment was conducted to obtain aged samples with 0, 60 and 120 aging cycles in accordance with the accelerated aging test protocol for wood materials. The results indicate that pine combustion involves three distinct thermal stages: pyrolysis, smouldering, and flaming, with critical high-risk transition points identified. Aging intensified fire risk and related hazards across all stages, particularly accelerating flame spread on vertical components.

KEYWORDS: Ancient timber structure, fire risk, smoke and heat hazards, combustion characteristic, wood aging.

## INTRODUCTION

Long-term natural aging, caused by exposure to sunlight, wind, and rain, coupled with intensified human activities such as the use of fire and electrical facilities, degrades wooden components and enhances their fire susceptibility. Fire incidents not only result in irreversible cultural and economic losses but also pose severe environmental hazards, making the research on wood combustion a central theme in fire science (Fang et al. 2001, Zhang et al. 2025, Gao et al. 2025). Previous studies have confirmed that moisture content, heating conditions, and intrinsic wood properties significantly affect combustion behaviour. Hedayati et al. (2018) noted that moisture content and external heating jointly regulate wood pyrolysis, while Richter et al. (2021) further validated thermal radiation intensity and oxygen concentration as key determinants of combustion processes. Critical parameters including heat release rate (HRR), mass loss rate (MLR), and smoke production rate (SPR) are essential for evaluating combustion performance. Xu et al. (2024) found that hardwoods and softwoods differ in the occurrence of secondary HRR peaks and charring rates, and Jin et al. (2024) demonstrated that $SnO_2$ coatings mitigate fire hazards by improving char porosity. However, discrepancies in testing methodologies lead to variations in the derived parameters of different studies.

Aging modifies wood's chemical properties (e.g., degradation of cellulose and lignin) and physical characteristics (e.g., porosity and density), which in turn alter its combustion performance. Long et al. (2024) and Deng et al. (2023) both confirmed that long-term natural aging impairs wood thermal stability and lowers ignition temperature; building on this. Liu et al. (2024) simulations using Fire Dynamics Simulator (FDS) further indicated that aging accelerates fire spread in ancient timber structures. Nevertheless, research on how aging affects combustion across the three typical stages (pyrolysis, smouldering, and flaming) remains insufficient, creating a research gap in this field.

Fire-derived smoke poses severe environmental and human health risks, yet existing studies mainly focus on wildfires, overlooking the substantial smoke and heat hazards posed by large-scale ancient timber buildings. Conventional cone calorimeters, a common testing tool, are unable to adjust oxygen concentration, a key factor in wood combustion, or capture aging's influence on fire propagation trends. To address these limitations and fill the aforementioned research gap, this study employs a fire propagation apparatus (FPA) to investigate the effects of aging on the combustion behaviour of pine wood, a material commonly used in ancient timber structures. The findings provide critical data for fire development modelling, fire spread prediction, and hazard assessment, which is of great significance for fire risk management and emergency planning of ancient timber buildings.

## MATERIAL AND METHODS

### Artificial accelerated aging

The pine wood specimens used in the experiment were obtained from a fast-growing plantation in North China. The tree species is 20-year-old Masson pine. The wood was sound, free of knots, decay, and insect damage. The specimens were machined to the specified dimensions and conditioned to the equilibrium moisture content under standard environmental conditions prior to combustion tests. Specimens from the same batch were inspected to ensure no discoloration, defects, or decay, thereby eliminating errors caused by material heterogeneity.

Artificial accelerated aging was conducted using a xenon-arc weathering chamber (ZH-HXD-225P) in accordance with ISO 4892-3 and ASTM D4329 standards, to simulate sunlight-induced photodegradation of ancient timber components. Key parameters were set as follows: irradiance 0.89 W/m², black panel temperature 60°C, condensation temperature 50°C, and rainfall duration 0.5 h per cycle. Each 12 h cycle included 8 h of continuous irradiation at the set black panel temperature and 4 h of light-free condensation. Two aging groups were established: 60 cycles (720 h total, labelled AC60) and 120 cycles (1440 h total, labelled AC120), representing different aging degrees.

**FPA test**

Combustion and fire spread tests were performed using FPA in compliance with ISO 12316 and ASTM E2058. By adjusting radiant heat flux (HF) and oxygen concentration (OC), the FPA simulates diverse fire scenarios, facilitating quantitative analysis of thermal and smoke hazards of aged pine.

Specimens were placed horizontally (100×100×10 mm) in aluminium holders for combustion tests and vertically (300×100×10 mm) on a dedicated frame for fire spread tests. The FPA comprises two core subsystems: a combustion control subsystem and a combustion product measurement subsystem. The holder or vertical frame was mounted on a load cell to continuously record mass loss during combustion, while a quartz-glass enclosure surrounds the specimen to form a combustion chamber with stable conditions. Four infrared heaters were uniformly arranged around the chamber to provide radiant heat, and airflow was introduced via a lower inlet to create a controlled convective environment.

All combustion products, together with supply air, were drawn through an exhaust duct into the measurement subsystem, where a Pitot tube, thermocouples, and laser sensors measured flow rate, temperature, and extinction coefficient. A small portion of the exhaust gas was diluted, filtered, and dried before entering a gas analyser for real-time detection of $O_2$, CO, and $CO_2$ concentrations. Heat release rate (HRR) was calculated based on oxygen consumption calorimetry principles. Tests were conducted under forced convection: oxygen concentration (0-21%) was adjusted by blending nitrogen and air, and external radiant heat flux was varied between 25 kW/m² and 40 kW/m². The experimental setup is shown in Fig.1, and each data point is the average of eight independent measurements.

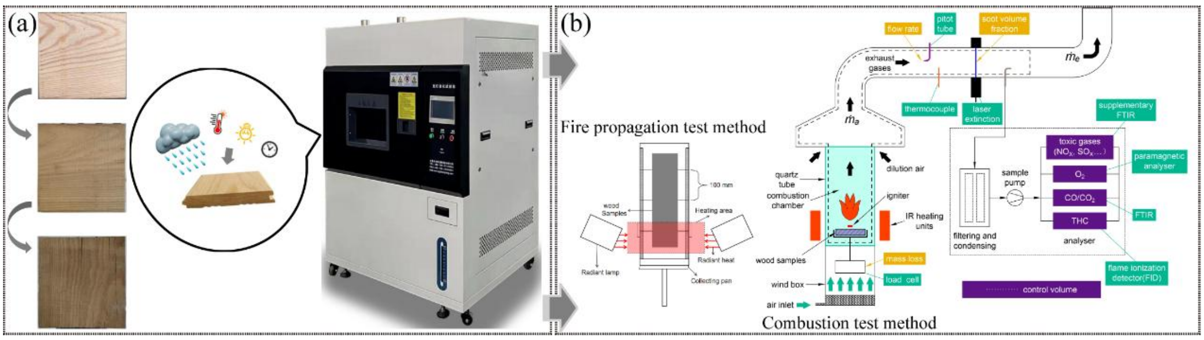


*Fig. 1: Schematic diagram of experimental method: (a) artificial accelerated aging method, (b) fire propagation apparatus (FPA) method.*

## RESULTS AND DISCUSSION

**Thermal behaviour characteristics of untreated pine wood**

When heated, untreated pine first undergoes pyrolysis, during which cellulose, hemicellulose and lignin decompose to release combustible gases (e.g., CO, $CH_4$) and tar (Di Blasi 2009). Throughout this stage, no visible flames or heavy smoke were observed, only surface discoloration, minor cracks, and negligible subsurface changes (Fig. 2a1-a3). Once the ignition temperature is reached, the pyrolysis gases oxidize vigorously, initiating flaming combustion—the most active stage of the entire combustion process. White ash then forms on the residual char, accompanied by significant sample shrinkage, fragmentation, and structural collapse (Fig. 2b1-b3).

As volatile gases become depleted or oxygen grows limited, the char layer oxidizes slowly to enter the smouldering stage, a flameless reaction between solid carbon and oxygen that releases smoke and heat. Notably, under low oxygen conditions, pine may skip the flaming stage and shift directly from pyrolysis to smouldering (Zhang et al. 2023), a process that affects approximately 50% of the specimen volume and produces more smoke than pyrolysis (Fig. 2c1-c3). As illustrated in the graph (Fig. 2), pyrolysis dominates under 0-15% $O_2$ across the 25-40 kW/m² radiation range, with weak dependence on radiation intensity. Smouldering, by contrast, requires 3-15% $O_2$ and 35-40 kW/m² radiation and this radiation demand becomes more pronounced under oxygen deficiency. Flaming combustion, meanwhile, necessitates ≥15% $O_2$: sufficient oxygen can sustain it even at low radiation, while 15-17% $O_2$ requires 37-40 kW/m² radiation, confirming oxygen as its dominant influencing factor.

In summary, below 15% $O_2$, higher radiation is required to trigger flaming combustion; insufficient radiation will only induce pyrolysis or smouldering. Conversely, at 25 kW/m², elevated oxygen levels can still sustain flaming combustion. Three critical transition points exist (Fig. 2, stars), where minor environmental fluctuations trigger shifts between these combustion states, thereby significantly increasing fire risk.

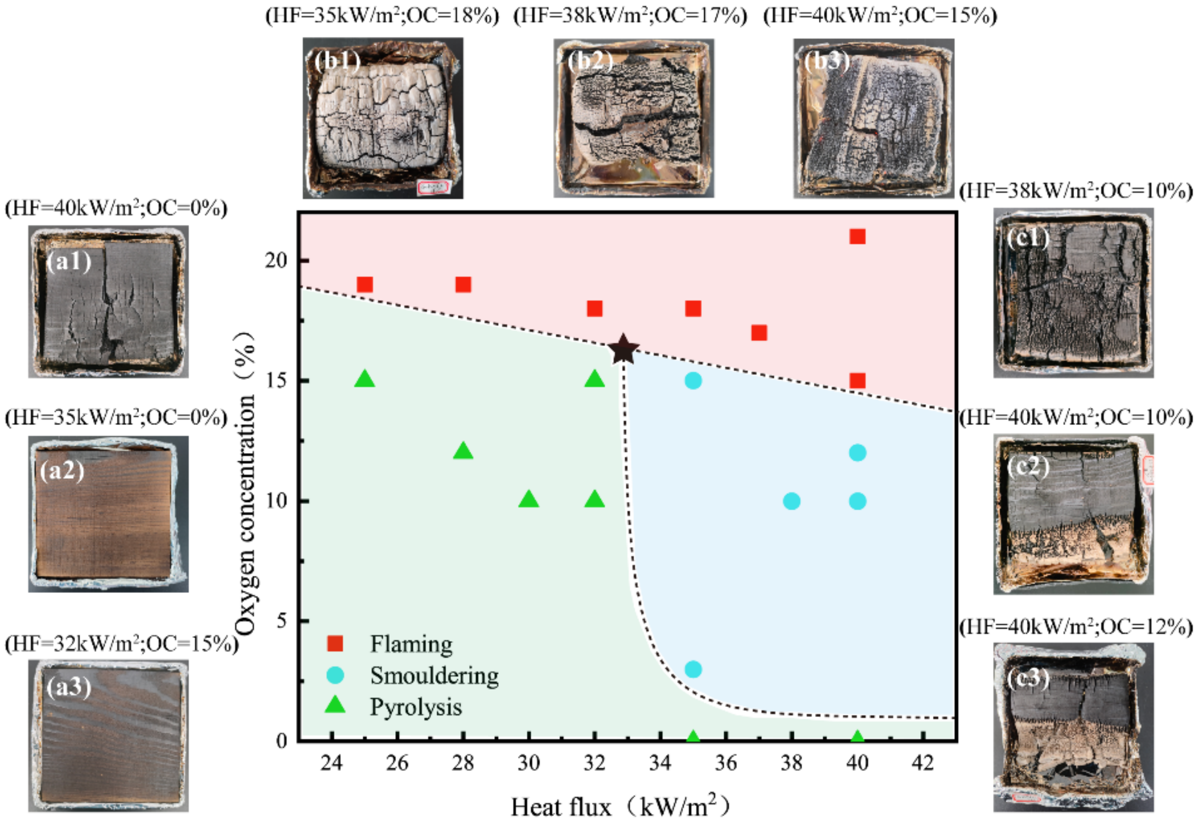


*Fig. 2: Influence of oxygen concentration and heat flux on the thermal behaviour of common pine wood.*

Heat release rate (HRR) is critical for evaluating thermal hazards and fire risk (Chow 2002), with curves for pine's three combustion states (pyrolysis, smouldering, flaming) shown in Fig. 3a1-c1. Consistent with earlier analysis, pyrolysis and smouldering have much lower HRR than flaming combustion, matching their less intense reactions. Pyrolysis HRR relies on endothermic-exothermic balance: macromolecule decomposition absorbs heat, while late-stage secondary oxidation of products may release slight heat. Only under high radiation (40 kW/m²) and oxygen-free conditions does HRR rise slightly, accelerating heat release and pushing flammable gas toward ignition threshold. Endothermic reactions dominate other pyrolysis conditions, keeping HRR near zero.

Smouldering HRR reflects char layer oxidation rate (Anca-Couce et al. 2012), with low, smooth fluctuations due to slow kinetics. Though low, its prolonged duration accumulates heat, potentially inducing adjacent material pyrolysis or reignition. Moderate oxygen (10-12%) and medium-high radiation (35-38 kW/m²) enhance char oxidation, temporarily boosting HRR before accelerated char consumption causes a decline. As the most active stage, flaming combustion has an HRR an order of magnitude higher, showing a bimodal pattern from delayed surface-inner heat transfer. Peak HRR varies slightly, co-regulated by radiation and oxygen: higher radiation shortens preheating via accelerated pyrolysis, while oxygen governs ignition timing. This confirms high-radiation pyrolysis elevates thermal hazard by shortening flaming ignition delay. Smoke production rate (SPR) is another key hazard indicator, with curves shown in Fig. 3a2-c2. Due to flameless incomplete oxidation, smouldering has the highest SPR from unoxidized carbon particles. At low oxygen, higher radiation (40 vs 35 kW/m²) intensifies char oxidation and pore blockage, boosting smoke-confirming radiation dominates smouldering SPR.

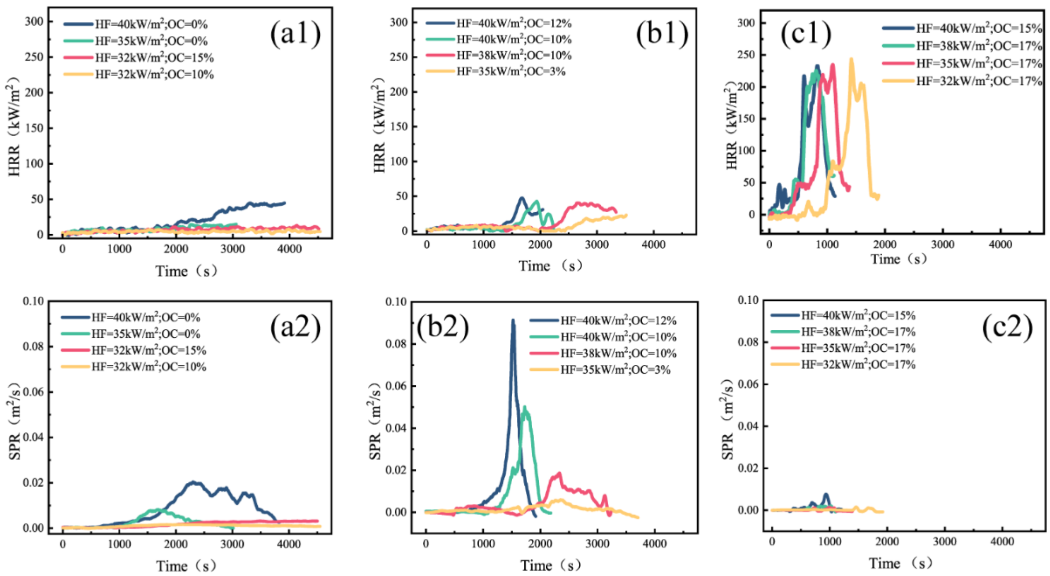


*Fig. 3: HRR and SPR of common pine wood during combustion under various thermal behaviors: (a) pyrolysis, (b) smouldering, (c) flaming.*

For pyrolysis, SPR rises as oxygen drops below 15%, as insufficient oxygen inhibits product oxidation and promotes tar condensation into smoke. Radiation also affects SPR: higher radiation accelerates pyrolysis to increase instantaneous SPR, while low radiation prolongs reaction and may raise total smoke despite lower instantaneous values. Flaming combustion has the lowest SPR due to complete volatile combustion. Only under high radiation (40 kW/m²) and moderate oxygen (15%) does SPR rise slightly, from incomplete combustion, highlighting oxygen as the governing factor for flaming SPR, unlike radiation-dominated smouldering.

CO toxicity and $CO_2$ asphyxiant effects further amplify fire hazards. Consistent with the aforementioned combustion behaviours, CO production rate (COP) and $CO_2$ production rate ($CO_2P$) of pine across the three states are shown in Fig. 4, with $CO_2P$ exceeding COP in all thermal stages.

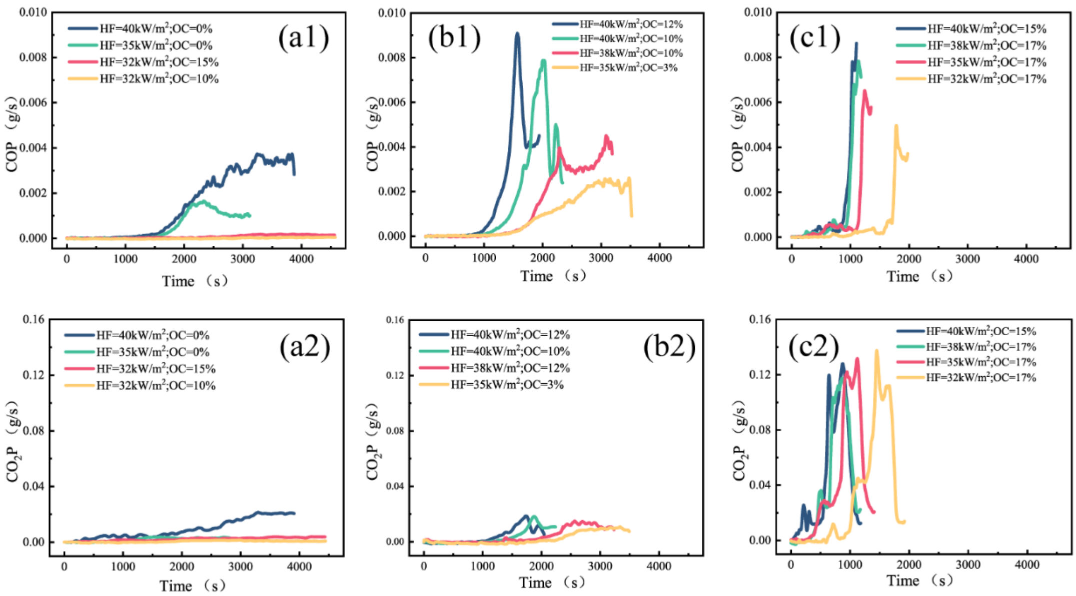


*Fig. 4: COP and $CO_2P$ of common pine wood during combustion under various thermal behaviours: (a) pyrolysis, (b) smouldering, (c) flaming.*

For pyrolysis, COP and $CO_2P$ are strongly regulated by radiation intensity. Higher radiation accelerates pyrolysis to boost COP, while also promoting levoglucosan decarboxylation and increasing $CO_2P$. Trace oxygen (≥0.5%) oxidizes CO to $CO_2$ via homogeneous and heterogeneous reactions (Li et al. 2009). When oxygen approaches 15% under low radiation, localized micro-oxidation converts CO to $CO_2$—aligning with pyrolysis' endothermic-dominated nature—slightly raising $CO_2P$ as COP nears zero. Smouldering COP and $CO_2P$ (Fig. 4b1-b2) increase with high radiation and moderate-to-high oxygen, governed by the balance between oxygen diffusion and char oxidation rate. Intensified reactions elevate both rates, but accelerated char oxidation (as observed earlier) causes pore blockage and local oxygen deficiency, further boosting COP. Lower radiation enables uniform char oxidation, raising $CO_2P$ and its proportion in exhaust gas—consistent with smouldering's stable reaction kinetics.

Flaming combustion, the most active stage, shows a marked $CO_2P$ rise, with its curve mirroring HRR (Fig. 4c2)—reflecting dominant complete carbon oxidation (Eq. 1), the most exothermic step (Chauhan et al. 2012, Yu et al. 2019). Sufficient oxygen enhances heat release, making $CO_2P$ a direct HRR indicator. COP peaks after HRR attenuation, signalling postflaming smouldering, with minimal CO from incomplete combustion. Overall COP variation is insignificant, emphasizing that smouldering poses persistent gaseous toxicity risk regardless of visible flames:

$$C + O_2 \rightarrow CO_2 \quad \Delta H \approx -353.9KJ/mol \tag{1}$$

**Effects of aging**

Aging significantly enhances pine's combustion hazards, with HRR, SPR, COP, and $CO_2P$ all increasing with aging degree, and their peak times advancing across all three combustion stages (pyrolysis, smouldering, flaming). UV irradiation drives these changes: it cleaves lignin and cellulose into low-molecular-weight compounds (reduced thermal stability, rapid decomposition, more volatiles) and induces surface microcracks and pores, which enhance oxygen diffusion, boost volatile combustion, and elevate HRR (Hosseinnezhad et al. 2019). SPR rises via phenoxy radical chain reactions and metal oxide ($Fe_2O_3$, $MnO_2$) catalysis, with oxygenated compounds condensing into smoke particles (Masto et al. 2015, Kalembkiewicz et al. 2018, Hiskia et al. 2001).

Aging-induced carboxyl and carbonyl groups favour decarboxylation (Eq. 2), raising $CO_2P$ (He et al. 2013). Microcracks cause uneven oxygen distribution, facilitating incomplete combustion (Eq. 3) and water-gasification (Eq. 4) to increase COP. Metal ions ($K^+$, $Ca^{2+}$) catalyse CO-to-$CO_2$ conversion (Eq. 5) (Lu et al. 2012), but oxygen diffusion limitations result in simultaneous rises in COP and $CO_2P$:

$$RCOOH \rightarrow CO_2 + RH \tag{2}$$
$$C + \frac{1}{2}O_2 \rightarrow CO \tag{3}$$
$$C + H_2O \rightarrow CO + H_2 \tag{4}$$
$$2CO + O_2 \xrightarrow{catalyze} 2CO_2 \tag{5}$$

In pyrolysis (Fig. 5), SPR increases far less than other parameters. Oxygen-containing groups favour decarboxylation (reducing tar condensation), and ash metal ions catalyse volatile oxidation to decompose tar precursors into gases (Cheng et al. 2020, Li et al. 2000). Thus, pyrolysis toxicity of aged pine is dominated by elevated CO and $CO_2$ emissions.

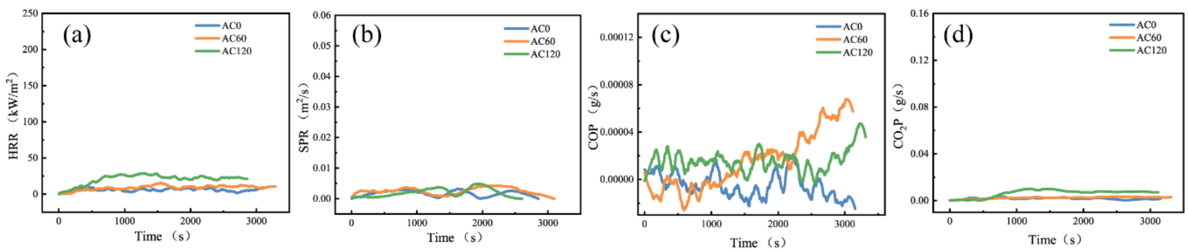


*Fig. 5: Effect of aging degree on pine pyrolysis: (a) HRR (b) SPR (c) COP (d) $CO_2P$.*

In smouldering (Fig. 6), all parameters rise, but HRR growth is mild, meaning smoke and toxic gas hazards outweigh thermal risks. Aging increases char porosity, lowering thermal conductivity to restrict HRR while enlarging surface area to release ultrafine carbon particles

(Wang et al. 2014). Pore oxygen deficiency induces CO formation, surface oxidation yields $CO_2$, and ash metal catalysis accelerates gas production without boosting HRR (Wang et al. 2021).

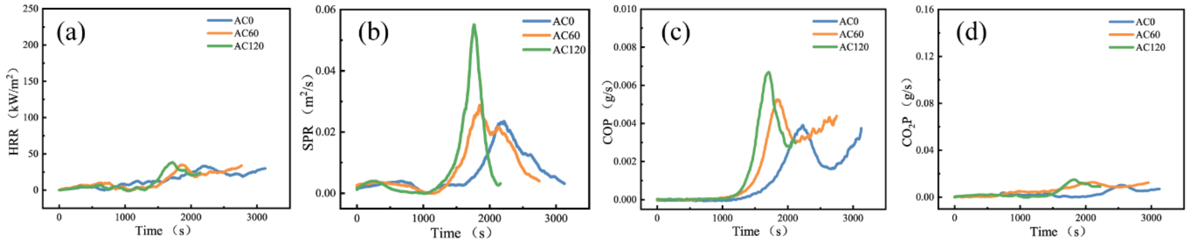


*Fig. 6: Effect of aging degree on pine smouldering: (a) HRR (b) SPR (c) COP (d) $CO_2P$.*

In flaming combustion (Fig. 7), parameter increases are most significant (absolute values peak). Low-molecular-weight volatiles from aging burn rapidly, and microcracks form oxygen diffusion channels to enhance combustion efficiency (Parker et al. 2015). Phenoxy radicals and reduced polar groups promote smoke formation; sufficient oxygen raises $CO_2P$, while transient pore oxygen deficiency and high-temperature gasification increase COP (Verhoeven et al. 2013).

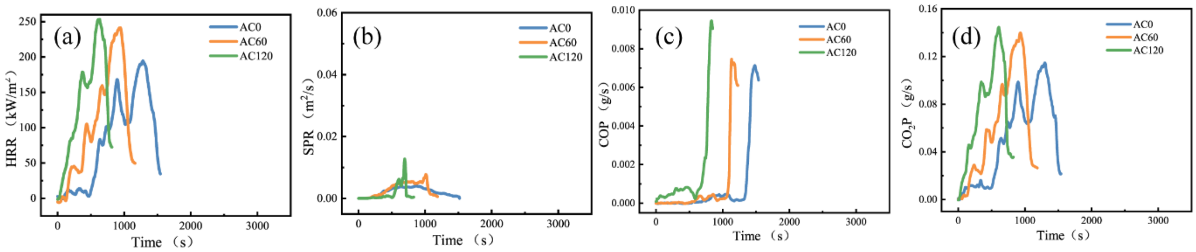


*Fig. 7: Effect of aging degree on pine flaming: (a) HRR (b) SPR (c) COP (d) $CO_2P$.*

Peak advancement stems from degraded thermal stability (shorter pre-pyrolysis period), radiative heat feedback (self-accelerating combustion), and porosity-enhanced oxygen diffusion-shifting kinetics to diffusion control and enabling earlier peak reaction rates (EL-Sayed et al. 2023).

**Fire spread characteristics**

Aging significantly enhances pine's fire and smoke-thermal hazards, and this effect is further amplified in vertical combustion, a typical flame propagation pathway in historic buildings. Aging's influence on vertical combustion parameters is shown in Fig. 8, consistent with the aforementioned combustion laws.

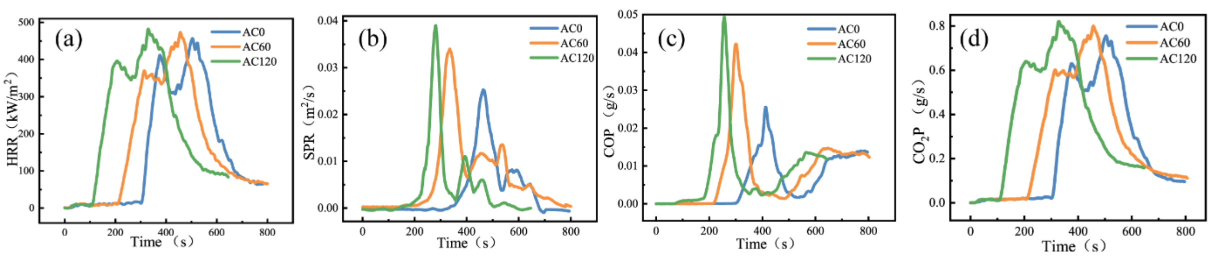


*Fig. 8: Effects of aging on the fire propagation characteristic parameters of pine wood.*

During vertical combustion, aging barely affects HRR and $CO_2P$ peak values but advances their peak timing with increasing aging degree. Upward flame propagation drives convective currents, drawing sufficient oxygen to maintain high combustion efficiency, mirroring fresh pine's oxygen-dependent flaming behaviour. Aging-induced porosity and microcracks (discussed earlier) enhance oxygen penetration, accelerating combustion and advancing peaks, while sufficient oxygen stabilizes peak magnitudes by keeping efficiency near theoretical maximum (Lo Basso et al. 2017).

By contrast, aging markedly elevates and advances SPR and COP peaks. Microcracks and pores facilitate longitudinal volatile release, forming dense combustible gas clouds. Concurrent oxygen demand for flame propagation and volatile oxidation causes local transient oxygen deficiency, exacerbating aged pine's incomplete combustion tendency, while aging-introduced metal ashes (e.g., $K^+$) preferentially catalyse volatile conversion to CO (Eq. 6), further boosting CO production:

$$CH_3CHO \xrightarrow{K^+} CO + CH_4 \tag{6}$$

Vertical burning amplifies aging effects (Shan et al. 2017): the char layer forms a longitudinal fibrous structure with gravity-aligned pores, enhancing upward oxygen diffusion but restricting lateral volatile dispersion. This heterogeneous gas mixing intensifies smoke and CO generation, building on aged pine's inherent smoke and toxic gas hazards. Radiant heat from lower char layers triggers self-accelerating combustion, and aged pine's reduced thermal conductivity (noted earlier) concentrates surface heat, further advancing peak timings.

The Fire Propagation Index (FPI), a key flame spread metric (Zhu et al. 2023) (units: $m^{5/3}/kW^{2/3}s^{1/2}$), is calculated via Eq. 7:

$$FPI = 750\left(\dot{Q}_{chem}/W\right)^{1/3} TRP^{-1} \tag{7}$$

where: $\dot{Q}_{chem}$ is peak chemical HRR (kW), W is specimen width (m), and TRP (thermal response parameter) reflects ignition resistance.

FPI values vary minimally with aging (AC0: 55.5; AC60: 59.5; AC120: 62.9). Vertical combustion shortens burning duration but barely affects HRR—aligning with stable peak HRR in aged pine's flaming combustion. Aging temporarily increases effective width W via microcracks but later reduces it due to loose, shedding char (Figs. 10b-d), offsetting HRR and TRP effects to keep FPI fluctuations small. Per FM Global guidelines (Tewarson et al. 1994), FPI > 20 indicates accelerated flame spread, all samples exceed this threshold, with aging further raising risk. Moderate aging increases FPI by 4.67% vs fresh pine, severe aging by 7.09% vs moderate aging, and 12.10% vs fresh pine (exceeding experimental uncertainty). FPI growth intensifies with aging degree, suggesting a threshold for substantial fire propagation risk elevation, consistent with aging's cumulative combustion hazard effect.

## CONCLUSIONS

This study explores the combustion behaviour of historic timber pine, focusing on aging effects and fire hazards via artificial photoaging and FPA experiments. Key conclusions are as follows: *(1)* Unaged pine exhibits three combustion states (pyrolysis, smouldering, flaming) with high-risk critical transition points. Flaming poses the greatest smoke-heat hazards; high-radiation pyrolysis and smouldering act as flaming precursors, as pyrolysis converts to flaming upon oxygen supply and smouldering heat induces adjacent combustion. *(2)* Pyrolysis has low HRR (easily overlooked) but generates combustible gases that may deflagrate with sudden oxygen input, requiring close monitoring. Smouldering features high smoke/CO concentrations, alongside persistent heat and re-ignition potential. Flaming triggers complete oxidation, boosting heat/$CO_2$ levels and asphyxiation risk, thus demanding rapid intervention. *(3)* Photoaging modifies pine's chemical and physical structure, enhancing volatility, oxygen penetration, and catalytic ash content. This elevates HRR (up to 135.31%), SPR, COP, $CO_2$P, and thermal-toxic risks. For smouldering, toxicity outweighs thermal hazards (SPR/COP/$CO_2$P up 34.33%/54.56%/44.83%, HRR up 15.46%), while flaming shows the largest parameter increases with advanced peaks, forming a "high-release, early-peak" pattern. *(4)* Severe aging promotes flame spread, particularly vertical combustion (high efficiency yet elevated hazard). Optimized oxygen convection stabilizes HRR/$CO_2$P peaks but accelerates burning; oxygen-volatile competition doubles toxicity via increased smoke/CO, underscoring the need for strategies balancing combustion control and toxic product suppression.

## ACKNOWLEDGMENTS

Supported by Guangdong S&T Programme (2025B0909040002, 2023A1111120002), Natural Science Foundation of Hebei Province (E2023507001), National Natural Science Foundation of China (51804314).

## REFERENCES

1. Fang, D.P., Iwasaki, S., Yu, M.H., Shen, Q.P., Miyamoto, Y., and Hikosaka, H., 2001: Ancient Chinese timber architecture. II: Dynamic characteristics. Journal of Structural Engineering 127(11): 1358-1364.
2. Zhang, B.Z., Chen, Y.X., Song, X.B., and Lu, Y., 2025: Fire hazard analysis and fire resistance evaluation of historic timber buildings based on multiple fire scenarios. International Journal of Architectural Heritage 19(11): 2944-2958.
3. Gao, Y., Song, X.B., and Peng, Y.Q., 2025: Experimental study on fire resistance of post-beam timber frames with traditional mortise-tenon joints with damage. Engineering Structures 333: 120165.
4. Hedayati, F., Yang, W.X., Zhou, A.X., 2018: Effects of moisture content and heating condition on pyrolysis and combustion properties of structural fuels. Fire and Materials 42(7): 741-749.
5. Richter, F., Jervis, F.X., Huang, X.Y., Rein, G., 2021: Effect on oxygen on the burning rate

of wood. Combustion and Flame 234: 111591.
6. Xu, L., Song, X.K., Li, S.C., Yu, J.B., Qi, Y.F., Zhang, Y., Hong X.C., 2024: Effect of different boundary conditions on the combustion properties and fire characteristics of typical woods. Energy 307: 132696.
7. Jin, E., Chung, Y.J., 2024: Evaluation of combustion characteristics for wood specimens coated with metal oxides of different oxidation states in the secondary stage of combustion (II). Wood Science and Technology 58(1): 253-271.
8. Long, M.T., Yi, L., Yan, L., Xu, Z.S., Zheng, J.X., 2024: Comparative analysis of microstructure, combustion characteristics and mechanical properties of *Pinus massoniana* lamb. under natural aging conditions. Thermal Science and Engineering Progress 48: 102425.
9. Deng, J., Liu, T.S., Yao, M., Yi, X., Bai, G.X., Huang, Q.R., Li, Z., 2023: Comparative study of the combustion and kinetic characteristics of fresh and naturally aged pine wood. Fuel 343:127962.
10. Liu, T.S., Li, A., Yao, M., Deng, J., Huang, Q.R., Li, Z., Li, H.J., Yi, X., 2024: Fire behavior characteristics and computational simulation research on historic wooden structures. Fire-Switzerland 7(12):478.
11. Di Blasi C., 2009: Combustion and gasification rates of lignocellulosic chars. Progress in Energy and Combustion Science 35(2): 121-140.
12. Zhang, Z.Y., Ding, P.F., Wang, S.P., Huang, X.Y., 2023: Smouldering-to-flaming transition on wood induced by glowing char cracks and cross wind. Fuel, 352:129091.
13. Chow, W.K., 2002: Assessment on heat release rate of furniture foam arrangement by a cone calorimeter. Journal of Fire Science 20(4): 319-328.
14. Anca-Couce, A., Zobel, N., Berger, A., Behrendt, F., 2012: Smouldering of pine wood: Kinetics and reaction heats. Combustion and Flame 159(4): 1708-1719.
15. Li, Q.Z., Zhao, C.S., Chen, X.P., Wu, W.F., Li, Y.J., 2009: Comparison of pulverized coal combustion in air and in $O_2/CO_2$ mixtures by thermo-gravimetric analysis. Journal of Analytical and Applied Pyrolysis 85(1-2): 521-528.
16. Chauhan, B., Kumar, N., Cho, H., 2012: A study on the performance and emission of a diesel engine fueled with Jatropha biodiesel oil and its blends. Energy 37(1): 616-622.
17. Yu, B., Tawiah, B., Wang, L.Q., Yuen, A.C.Y., Zhang, Z.C., Shen, L.L., Lin, B., Fei, B., Yang, W., Li, A., 2019: Interface decoration of exfoliated MXene ultra-thin nanosheets for fire and smoke suppressions of thermoplastic polyurethane elastomer. Journal of Hazard Materials 374: 110-119.
18. Hosseinnezhad, S., Zadshir, M., Yu, X.K., Yin, H.M., Sharma, B.K., Fini, E., 2019: Differential effects of ultraviolet radiation and oxidative aging on bio-modified binders. Fuel 251: 45-56.
19. Masto, R.E., Sarkar, E., George, J., Jyoti, K., Dutta, P., Ram, L.C., 2015: PAHs and potentially toxic elements in the fly ash and bed ash of biomass fired power plants. Fuel Processing Technology 132: 139-152.
20. Kalembkiewicz, J., Galas, D., Sitarz-Palczak, E., 2018: The physicochemical properties and composition of biomass ash and evaluating directions of its applications. Polish Journal of Environmental Studies 27(6): 2593-2603.

21. Hiskia, A., Mylonas, A., Papaconstantinou, E., 2001: Comparison of the photoredox properties of polyoxometallates and semiconducting particles. Chemical Society Reviews 30(1): 62-69.
22. He, C., Giannis, A., Wang, J.Y., 2013: Conversion of sewage sludge to clean solid fuel using hydrothermal carbonization: Hydrochar fuel characteristics and combustion behavior. Applied Energy 111: 257-266.
23. Lu, X., Ren, W., Wu, G., 2012: $CO_2$ copolymers from epoxides: Catalyst activity, product selectivity, and stereochemistry control. Accounts of Chemical Research, 45(10): 1721-1735.
24. Cheng, R.X., Qi, C.R., Wang, L., Xiong, W.F., Liu, H.J., Jiang, H.F., 2020: Visible light-promoted synthesis of organic carbamates from carbon dioxide under catalyst- and additive-free conditions. Green Chemistry 22(15): 4890-4895.
25. Li, C.Z., Sathe, C., Kershaw, J.R., Pang, Y., 2000: Fates and roles of alkali and alkaline earth metals during the pyrolysis of a Victorian brown coal. Fuel 79(3-4): 427-438.
26. Wang, H., Li, Y.W., Zhu, T.B., Sang, S.B., Wang, Q.H., 2014: Microstructures and mechanical properties of $Al_2O_3$-C refractories with addition of microcrystalline graphite. Ceramics International 40(7): 11139-11148.
27. Wang, Y.S., Chen, Y., Liang, X.Y., Tan, P.Q., Deng, S.L., 2021: Impacts of lubricating oil and its formulations on diesel engine particle characteristics. Combustion and Flame 225: 48-56.
28. Parker, D.S.N., Kaiser, R.I., Troy, T.P., Kostko, O., Ahmed, M., Mebel, A.M., 2015: Toward the oxidation of the phenyl radical and prevention of PAH formation in combustion systems. Journal of Physical Chemistry A 119(28): 7145-7154.
29. Verhoeven, L.M., Oliveira, M.H.D., Lantz, A., Li, B., Li, Z.S., Luijten, C.C.M., van Oijen, L.A., Alden, M., de Goey, L.P.H., 2013: A numerical and experimental study of Polycyclic Aromatic Hydrocarbons in a laminar diffusion flame. Proceedings of the Combustion Institute 34: 1819-1826.
30. EL-Sayed, S., Mostafa, M., 2023: Kinetics, thermodynamics, and combustion characteristics of Poinciana pods using TG/DTG/DTA techniques. Biomass Conversion and Biorefinery 13(13): 11583-11607.
31. Lo Basso, G., Nastasi, B., Garcia, D.A., Cumo, F., 2017: How to handle the Hydrogen enriched Natural Gas blends in combustion efficiency measurement procedure of conventional and condensing boilers. Energy 123:615-636.
32. Shan, F.P., Lin, Q.Z., Zhou, K., Wu, Y.K., Fu, W., Zhang, P., Song, L.B., Shao, C.Y., Yi, B.L., 2017: An experimental study of ignition and combustion of single biomass pellets in air and oxy-fuel. Fuel 188:277-284.
33. Zhu, T.H., Zhou, X., Guo, G.Z., Chai, Z.H., Gao, M., 2023: Synergistic flame retardant effect between ionic liquid functionalized imogolite nanotubes and ammonium polyphosphate in epoxy resin. Polymers 15(6): 1455.
34. Tewarson, A., 1994: Flammability parameters of materials: ignition, combustion, and fire propagation. Journal of Fire Science 12(4): 329-356.

TIANWEI ZHANG*[1,2], MINGZE BAI[1,2], HAO LIU[1,2], ZIDONG GUO[1], ZHIXIN TANG[2],
HAO CHANG[1], XIAORUI ZHANG[1,2]
[1]CHINA PEOPLE'S POLICE UNIVERSITY
[2]HEBEI KEY LABORATORY OF EMERGENCY RESCUE TECHNOLOGY
NO. 220 XICHANG ROAD, LANGFANG
CHINA
*Corresponding author: zhangtianwei@cppu.edu.cn